Trimethylethoxysilane Liquid-Phase Hydrolysis Equilibrium and Dimerization Kinetics: Catalyst, Nonideal Mixing, and the Condensation Route

Stephen E. Rankin, Ján Šefčík,† and Alon V. McCormick*

Department of Chemical Engineering and Materials Science, University of Minnesota, Minneapolis, Minnesota 55455

Received: January 25, 1999; In Final Form: March 24, 1999

Although the kinetics of organoethoxysilane hydrolytic (poly)condensation have been studied under kinetically simplified conditions, materials are actually synthesized from nonideal mixtures with high monomer and catalyst concentrations. Using ^{29}Si nuclear magnetic resonance, we study the hydrolysis of trimethylethoxysilane and the dimerization of the resulting silanol in aqueous ethanol at monomer and catalyst concentrations typical of organically modified silicate synthesis. Under acidic conditions, we find that when (and only when) the effects of solvent composition on catalyst activity are considered, it becomes clear that water-producing condensation is the dominant dimerization route. Under basic conditions, the extent of deprotonation of the weakly acidic silanol passes through a minimum during reaction, thereby producing an anomolous trend in reaction rate. This necessitates a kinetic model which is first order in *both* silanol and deprotonated silanol and which accounts for changing deprotonation.

Introduction

Hydrolytic polycondensation of alkoxysilanes, one type of sol−gel processing, is a materials processing technique of intense and growing interest.[1−3] This interest comes from researchers in a variety of fields including ceramics; inorganic, organic, and "materials" chemistry; polymer chemistry and physics; electronic materials; optical materials; and catalysis. Materials that can be synthesized by this technique include conventional metal oxide ceramics in novel shapes including thin films, coatings, and near net shapes; ceramics of these shapes and others containing highy dispersed organic modifiers; zeolites and related molecular sieves; disordered and ordered mesoporous silicates; amorphous silicone resins; low-dielectric silsesquioxanes; low-molecular-weight silicone oils and crystals; and monolayer films.

There is considerable interest in understanding and controlling the molecular structure of these silicates and organically modified silicates. Since quartz is the minimum-energy structure of silica at room temperature, both zeolites and the numerous amorphous silica structures (including biological and synthetic mesoscopically ordered silicates[4]) are metastable.[5] Their existence is governed by dynamic processes. Increased structure variability is introduced by organic modification. To understand how to manipulate siloxane structure through processing conditions, we must investigate the sometimes subtle interplay of all factors influencing the rates of processes contributing to structure evolution.

Previous investigations (including many in this journal[6−10]) have yielded many insights into the behavior of network-forming ethoxysilane precursors. However, the behavior of base-catalyzed and template-containing systems is complicated by phase behavior which depends not only on the overall solution composition but also on the distribution[11] of species present. The issue of phase separation can only be understood, however, once the chemical behavior of these systems has been addressed. To approach this, we start with simpler systems which do not display complicated phase behavior, here, the simplest possible system undergoing the same chemistry, i.e., the monofunctional alkoxysilane system.

This system undergoes the same chemistry as other alkoxysilanes. First, alkoxy groups are hydrolyzed (eq 1). The resulting silanols form siloxane bonds and a condensate−either water (eq 2) or alcohol (eq 3).

$$(CH_3)_3Si{-}OR + H_2O \rightarrow (CH_3)_3Si{-}OH + ROH \quad (1)$$

$$(CH_3)_3Si{-}OH + HO - Si(CH_3)_3 \rightarrow (CH_3)_3Si{-}O{-}Si(CH_3)_3 + H_2O \quad (2)$$

$$(CH_3)_3Si{-}OH + RO - Si(CH_3)_3 \rightarrow (CH_3)_3Si{-}O{-}Si(CH_3)_3 + ROH \quad (3)$$

Formerly,[12] we investigated the thermodynamics of these reactions in aqueous ethanol ($R = C_2H_5$) and found equilibrium coefficients near 15 for hydrolysis and 63 for water condensation. (The equilibrium coefficient for alcohol condensation is linearly dependent on these coefficients.) We also determined the deprotonation (eq 4) equilibrium coefficient K_d for trimethyl silanol to be about 10 at room temperature.

$$(CH_3)_3Si{-}OH + OH^- \overset{K_d}{\rightleftharpoons} (CH_3)_3Si{-}O^- + H_2O \quad (4)$$

Grubb[13] began investigating trialkylsilanol esterification and condensation behavior in alcohols using Karl Fischer titration. Unfortunately, this technique only gives a measure of the combined concentrations of silanol and water. This value does not allow one (without additional assumptions) to distinguish changes due to esterification and hydrolysis from those due to condensation, nor to determine the route by which condensation

* Corresponding author.
† Current address: 139-74 Beckman Institute, California Institute of Technology, Pasadena, CA 91125.

10.1021/jp990304b CCC: $18.00
Published on Web 05/11/1999

occurs. The technique also has the disadvantage that the sample must be disturbed by the titration, so artifacts may be introduced by shifting equilibria.

Kelling and coworkers studied in detail the kinetic behavior of organodimethylsilanols in dioxane/water and toluene/water.[14−17] They report, for instance, that triorganosilanol dimerization is second order with respect to silanol concentration with acid and first-order with respect to silanol concentration with base, and that condensation is usually first-order with respect to catalyst concentration. However, they consider conditions unusual for sol-gel processing (specifically, dioxane or toluene as solvent), and the characterization technique (gas chromatography) is invasive. What remains unclear is the role of the solvent under conditions more typical of sol−gel processing (where high concentrations of monomer and catalyst, and alcoholic solvents are common). Most notably, the competition between water- and ethanol-producing condensation has not been characterized for trimethylethoxysilane in aqueous ethanol.

Pohl and Osterholtz[18−20] performed elegant characterizations of the behavior of mono-, di- and trifunctional organosilanols in buffered aqueous solution by liquid-state nuclear magnetic resonance (NMR), a noninvasive technique. They find the expected linear dependence of condensation rate coefficient on the concentrations of both hydroxyl ion and hydronium ion.

It is to the credit of these previous investigators that they were able to devise experimental conditions in which specific trends could be isolated. This investigation builds upon the carefully controlled studies of the past to move into more complicated compositions. Usually, sol−gel processing is done in unbuffered solutions containing a good deal of ethanol (alcohol is frequently used as a cosolvent of the alkoxysilane and water initially, and more alcohol forms during reaction). With these conditions, the models applicable under controlled conditions may begin to break down. Ethanol and water alone mix nonideally, and hydrochloric acid activity is known to be a function at least of the ethanol-to-water ratio.[21] Also, silanols are weakly amphiprotic, so when the solution is not buffered, there might be shifts in overall pH (or more importantly, in the concentration of active species) which have the potential to change the course of reaction.

This paper focuses on how to distinguish the condensation route (alcohol- vs. water-producing), on nonideality of ethanol/water mixtures and on the effects of variable deprotonation of weakly acidic silanols. These issues are explored using ^{29}Si NMR—this nucleus is sensitive to shielding differences caused by both hydrolysis and condensation extents, and the technique is noninvasive.

Under acidic conditions, we will investigate the interdependent roles of catalyst and water content on condensation kinetics in mostly ethanol solutions. Three effects may contribute to changes with the ethanol-to-water ratio: (1) The effect of hydrolysis extent (due to water content) on the competition between water condensation (eq 2) and alcohol condensation (eq 3), and (2) the effect of hydrolysis extent on condensation reactivity, and (3) the effect of water content on the activity of the ionic and nonionic species present.

Since we have chosen a monofunctional system, the only effect of hydrolysis extent on condensation kinetics is the competition between condensation routes. A nearest-neighbor substituent effect (the second effect above) can be ruled out because the only ligands besides the reactive one are always methyl groups.

Grubb[13] assumed that alcohol-producing condensation between trimethylsilanol and trimethylalkoxysilanes dominates under acidic conditions, but this has not been independently verified and could not be proved by Karl Fischer titration alone. Assink and Kay[22] find for acid-catalyzed tetramethoxysilane that methanol-producing condensation competes with but does not dominate water-producing condensation. On the other hand, they report that ethanol-producing condensation is nearly negligible for tetraethoxysilane.[23] The route for trimethylethoxysilane remains unknown.

TABLE 1: Compositions Investigated

Name	$[TMES]_0$	$[H_2O]_0$ (M) {*W*}	Catalyst	$[catalyst]_0$ (M)
A-1	2.0	4.0 {2.0}	HCl	0.01
A-2	2.0	4.0 {3.0}	HCl	0.00316
A-3	2.2	4.4 {2.0}	HCl	0.0022
A-4	1.85	7.39 {4.0}	HCl	0.00226
A-5	1.85	11.1 {6.0}	HCl	0.00226
A-6	2.0	0.8 {0.4}	HCl	0.002
A-7	2.0	1.4 {0.7}	HCl	0.002
A-8	2.0	2.0 {1.0}	HCl	0.002
A-9	2.0	2.5 {1.25}	HCl	0.002
A-10	2.0	3.0 {1.5}	HCl	0.002
A-11	1.85	0.629 {0.34}	HCl	0.00226
A-12	1.85	1.48 {0.8}	HCl	0.00226
B-1	1.95	5.05 {2.6}	NaOH	0.029

The effect of water content on catalyst activity has not been considered in previous investigations of alkoxysilane chemistry. This issue may have been avoided by Assink and Kay in their study of tetraethoxysilane condensation[23] by working only at low extents of hydrolysis (only up to one-fourth water per ethoxyl group) and therefore always with a low free water content. We will find that accounting the for the effects of water on catalyst activity has a major influence on the interpretation of our kinetic experiments for the monofunctional system.

Under basic conditions, we will find that one cannot neglect ionization equilibria when modeling the reaction kinetics of trimethylethoxysilane. In other words, it is not possible to use a single effective rate coefficient at a certain pH (as we have often done in the past with acid catalyst). Instead, we must use a rate expression accounting for ionization equilibrium even to describe the changing rate of condensation over the course of a single experiment.

Experimental Section

The initial composition of each sample (after mixing) is listed in Table 1. Samples were prepared by first placing a solution of monomer and ethanol in a septum-capped NMR cell (a 5 mm o.d. glass tube) and by injecting an equal volume of a solution containing water and the desired catalyst to give the initial composition shown in the table. Solutions were prepared from trimethylethoxysilane [TMES] (≥98%, from Aldrich), ethanol (anhydrous grade, Aaper Alcohol & Chemical), filtered deionized water (prepared in house), and either a normalized hydrochloric acid solution (Aldrich) or a 1 N standardized sodium hydroxide solution prepared from filtered deionized water and solid NaOH (Aldrich). Chromium acetylacetonate (Aldrich), 1 wt %, was added as a paramagnetic relaxation agent[24] to the solvent ethanol. All experiments were conducted at room temperature (22 ± 0.2 °C).

Once samples were mixed and homogeneity visually confirmed, the samples were inserted into the spectrometer (within 5 min from mixing). ^{29}Si nuclear magnetic resonance (NMR) spectra were gathered using a Varian VXR-500 instrument with a broad-band probe operating at 99.309 MHz under quadrature detection. The number of transients per spectrum was at least eight but was increased when possible to improve the signal-

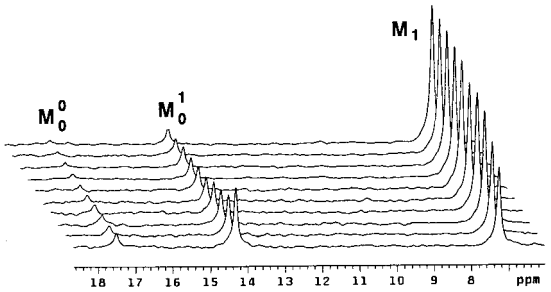

Figure 1. Representative ^{29}Si NMR spectra for reacting acidic trimethylethoxysilane system (sample A-1). The first spectrum was collected 2.1 min after mixing and $^4/_3$ min elapse between spectra. Chemical shifts are reported relative to external tetramethylsilane in a solution of ethanol with Cr(acac)$_3$. M_i^j represents a site with i siloxane bonds and j hydroxyl groups.

to-noise ratio. We waited 10 s between 60° radio frequency pulses to allow complete relaxation of the ^{29}Si nuclei. We verified that quantitatively similar results are obtained with a longer interpulse delay, confirming that the delay is long enough to provide quantitative data.

An external sample of tetramethylsilane in ethanol containing 1 wt % Cr(acac)$_3$ was used as a chemical shift standard. Because of the broad signal from the glass in the probe and NMR cell,[25] we collected spectra with a large spectral width (17 kHz) and with at least 32000 data points per spectrum. Exponential line broadening of 1−3 Hz was applied to each spectrum to maximize the signal-to-noise ratio. Decoupling at 500 MHz was gated on during acquisition and off otherwise (to avoid a possible negative NOE).

Results and Discussion

Acidic System. Figure 1 shows the ^{29}Si NMR spectra collected for a representative sample (A-1). The unhydrolyzed monomer peak (17.5 ppm) is assigned by comparison to a solution containing an identical concentration of TMES but without water. The dimer peak (7.3 ppm) is easily assigned as the monotonically growing peak, and the hydrolyzed monomer (14.3 ppm) appears after water is added but decays after reaching a maximum. These assignments closely match those of Suda et al.[26] (who also used ethanol as a solvent) and follow the same trend as those of Hook,[27] although they differ from the latter by up to +0.9 ppm, possibly because Hook's solutions contain a large concentration of d_6-acetone. The chemical shift trends do not change with composition, but the actual chemical shifts do depend slightly on composition, with a difference of up to +1 ppm observed for the unhydrolyzed monomer, up to +0.5 ppm for the hydrolyzed monomer (both with much higher water content, see the Appendix), and the dimer chemical shift changing little. The change in chemical shift is most likely due to the effects of the solvent composition.[28] The total integrated intensity of the spectra remains constant in this case and in all others except for one (sample A-5), which apparently goes through liquid−liquid phase separation at long times (see the Appendix).

Without exception in the range of hydrochloric acid-catalyzed conditions studied, hydrolysis pseudoequilibrium[29] is observed. This is characterized by the extent of hydrolysis reaching its equilibrium value before a significant condensation extent is reached (most often by the time the first spectrum was collected). For many cases this means that the fractional extent of hydrolysis $\{\chi = [\mathrm{SiOH}]/([\mathrm{SiOH}] + [\mathrm{SiOEt}])\}$ is nearly constant with respect to condensation extent. An example of this is shown in Figure 2 for sample A-1. For this sample the hydrolysis extent

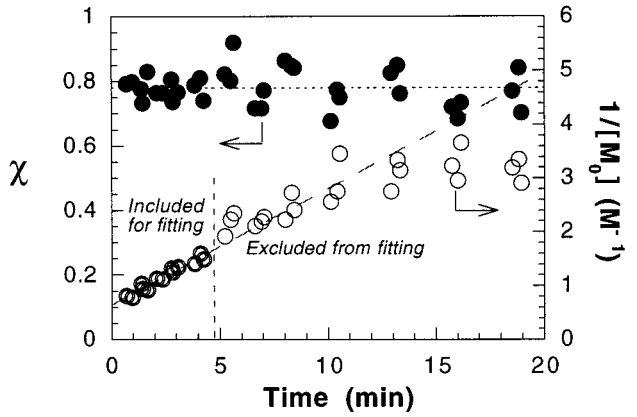

Figure 2. An example of the fitting to data of an acid-catalyzed sample (A-1). The hydrolysis extent is fit with a constant and the inverse monomer concentration is fit with a line. The data are taken from three identical experiments. The fitting is done using as many points as possible before excessive scatter and a deviation from linearity (due to reversibility) is observed.

(filled circles) is close to a constant value of 0.78 even at the first datum.

We have reported on the hydrolysis pseudoequilibrium behavior of these samples and other ethoxysilanes[30] and have always measured hydrolysis equilibrium coefficients in the range of 10−30. The pseudoequilibrium approximation is useful because it allows us to treat hydrolysis through algebraic rather than differential equations. It is challenging to determine the condensation route under hydrolysis pseudoequilibrium, however, because regardless of the route, the distribution of SiOEt and SiOH groups is "scrambled" as condensation proceeds:

$$(\mathrm{Me})_3\mathrm{SiOC_2H_5} + \mathrm{H_2O} \overset{\text{fast}}{\rightleftharpoons} (\mathrm{Me})_3\mathrm{SiOH} + \mathrm{C_2H_5OH} \quad (5)$$

Because water- and alcohol-producing condensation are nearly indistinguishable in a single experiment when hydrolysis pseudoequilibrium holds, we do not yet assume a route and instead use an effective condensation rate coefficient for each experiment, defined by:

$$\frac{\mathrm{d}[\mathrm{M_0}]}{\mathrm{d}t} = -k_{\mathrm{eff}}[\mathrm{M_0}]^2 \quad (6)$$

where $[M_0]$ is the concentration of all monomer (hydrolyzed or not) and we expect that contributions from water and alcohol condensation give $k_{\mathrm{eff}} = k_{\mathrm{cw}}\,\chi^2 + 2k_{\mathrm{ca}}\,\chi(1-\chi)$. Since χ is nearly constant for all experiments, k_{eff} is also nearly constant and could be found by fitting the solution of eq 6 to the experimental data.

The initial condition for condensation kinetics is ill-defined because there is some finite period of time required for the hydrolysis pseudoequilibrium to be established. However, the rate coefficient from the point of reaching hydrolysis pseudoequilibrium is not affected by this, so we solve eq 6 with a perturbation to the known initial monomer concentration accounting for this induction period, to find the following solution:

$$[\mathrm{M_0}]^{-1} = [\mathrm{M_0}]_0^{-1} + \epsilon + k_{\mathrm{eff}}\mathrm{t}$$

where ϵ is a constant which accounts for the induction time for hydrolysis pseudoequilibrium to be established. An example of the type of fit observed using this relationship is shown for sample A-1 in Figure 2. This result is typical: data from three separate experiments are shown and the correlation coefficient

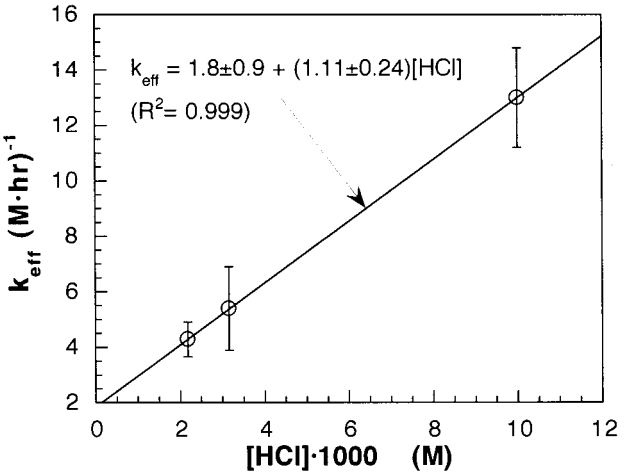

Figure 3. The effect of hydrochloric acid on the apparent condensation rate coefficient of hydrolyzed trimethylethoxysilane at 22 °C. The points shown are for samples with a pseudoequilibrium water concentration of about 2.8 M (A-1−A-3).

TABLE 2: Hydrolysis Equilibrium Values (χ_{eq} and $[H_2O]_{eq}$) and Effective Bimolecular Condensation Rate Coefficients[a] Measured for Acid-Catalyzed Systems

sample	χ_{eq}	$[H_2O]_{eq}$ (M)	k_{eff} (M h)$^{-1}$
A-1	0.78	2.82	13.0 ± 1.8
A-2	0.7	2.72	5.4 ± 1.5
A-3	0.79	3.15	4.3 ± 0.62
A-4	0.88	6.12	1.12 ± 0.065
A-5	0.91	9.67	1.65 ± 0.090
A-6	0.26	0.13	2.45 ± 0.27
A-7	0.45	0.47	3.07 ± 0.26
A-8	0.60	0.89	2.95 ± 0.24
A-9	0.64	1.28	2.03 ± 0.31
A-10	0.72	1.73	2.27 ±0.20
A-11	0.11	0.043	1.64 ± 0.28
A-12	0.45	0.576	2.12 ± 0.25

[a] All rate coefficients are found by linear regression, and error estimates are for 95% tolerence levels.

for the fit in Figure 2 is 0.97. For all samples, at least eight data points are used for the regression analysis and the set of points chosen starts from the point that χ is constant and stops when the linearity of the data deteriorates (usually because of increased scatter as the monomer concentration drops). This corresponds to following the decay of monomer to at least one half of its original concentration. Points where condensation reversibility becomes important (as determined by a clear drop in the slope of $[M_0]^{-1}$ vs time) are also excluded from the regression analysis.

Table 2 presents the measured fractional hydrolysis extent at pseudoequilibrium, water concentration at pseudoequilibrium, and effective bimolecular condensation coefficient for all of the acid-catalyzed samples. The water concentrations were found using the stoichiometry of the hydrolysis and condensation reactions, with site concentrations from the NMR spectra:

$$[H_2O] = [H_2O]_0 - [(CH_3)_3SiOH] - [\{(CH_3)_3Si\}_2O] \quad (7)$$

The error estimates in Table 2 are determined by standard analysis of the linear regression results.[31]

Some of the water concentrations in Table 2 are approximately equal (for samples A-1 to A-3), so it is possible to observe for those concentrations how the effective bimolecular condensation rate coefficient depends on acid concentration without concern about the effect of the water content. Figure 3 shows the results for these samples (all of about 2.8 M water at

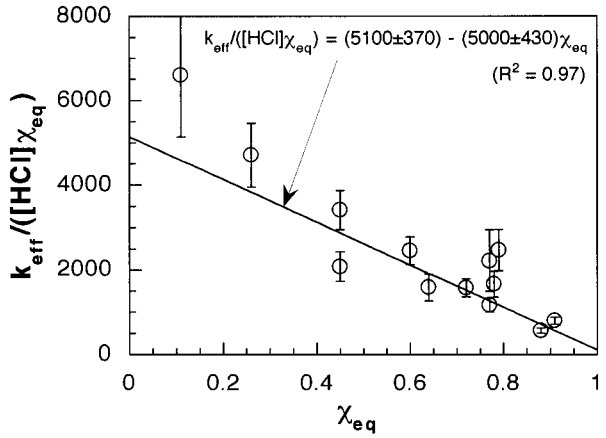

Figure 4. Results of fitting eq 12 to all measured experimental data. The fit was restricted so that the *x*-intercept is greater than or equal to 1 (the function fit is $y = m(1 - x) + \sqrt{b^2}$), and the estimated error of each point was used to weight the residual function.

hydrolysis pseudoequilibrium). As should be expected for homogeneous catalysis by a strong acid, we find that $k_{eff} \propto$ [HCl]. We might anticipate that this should be true regardless of the condensation route and Figure 3 gives no cause to doubt this. This dependence is easily explained by the following classic scheme:[14,20]

$$\equiv Si{-}OH + SH^+ \rightleftharpoons \equiv Si{-}OH_2^+ + S \quad (8)$$

$$\equiv Si{-}OH_2^+ + XO{-}Si \equiv \rightarrow \equiv Si{-}O{-}Si \equiv + XOH^+ \quad (9)$$

where S represents a proton-accepting solvent (either ethanol or water) and X is either a hydrogen or an ethyl group.

Assuming labile proton redistribution equilibrium (eq 8) and that eq 9 is the rate-limiting step, we can write:

$$\frac{d[SiOX]}{dt} = k^*[\equiv SiOH_2^+][\equiv SiOX]$$

$$= k^*\frac{K_p[\equiv Si - OH][HCl]}{[S] + K_p[\equiv Si - OH]}[\equiv SiOX]$$

$$= k'[HCl][\equiv SiOH][\equiv SiOX] \quad (10)$$

where K_p is the protonation redistribution equilibrium coefficient (for eq 8). Depending on X (H or R), k^* and k' apply to either alcohol- or water-producing condensation. In writing eq 10, complete dissociation of HCl is assumed ($[HCl] = [\equiv SiOH_2^+] + [SH^+]$), and for the last equivalence, it is assumed that [S] ∼ constant ≫ $K_p[\equiv Si\ {-}OH]$.[32]

To explore the effect of water concentration, we must consider not only the effect of water on the hydrolysis extent (and therefore on the condensation route) but also the effect of water on the activity of the cations present. The simplest hypothesis is that water content has no effect on activity coefficients. If this is the case we expect that

$$k_{eff} = [HCl]\{k'_{cw}\chi^2 + 2k'_{ca}\chi(1 - \chi)\} \quad (11)$$

which can be rearranged to give an expected linear relationship:

$$\frac{k_{eff}}{\chi} = [HCl]\{(k'_{cw} - 2k'_{ca})\chi + 2k'_{ca}\} \quad (12)$$

Figure 4 shows the results of fitting this functional form (slightly modified to ensure crossing the *x*-axis at ≥1) to all of

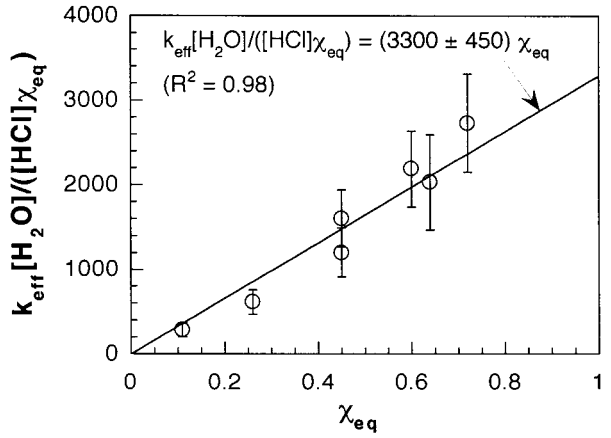

Figure 5. Fit of eq 14 to the subset of experimental data with low water content (samples A-6−A-12). Fitting is restricted so that the *y*-intercept is greater than or equal to zero (fitting function: $y = mx + \sqrt{b^2}$), and the estimated uncertainty of each coefficient was used to weight the residual function.

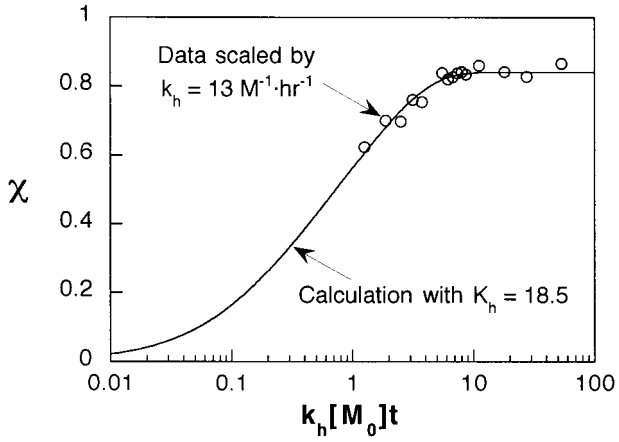

Figure 6. Plot of hydrolysis extent against dimensionless time. The data (points) were scaled using a value of $k_h = 13\ M^{-1}\ h^{-1}$, and the calculation (solid curve) was scaled using $K_h = 18.5$.

the measured rate coefficients. Estimated errors in the coefficients are used to weigh the residual function for fitting. From the values of the slope and intercept found, it appears that k_{cw} is on the order of 2% of the value of k_{ca}; in other words, this treatment of the data suggests that water-producing condensation is nearly negligible under most conditions.

However, Tourky et al. have investigated the variation of acidity (HCl activity) with water content in ethanol/water mixtures[34] and report that the protonation extent of *p*-nitroaniline is *not* constant but varies inversely with water concentration at low water concentrations (or in other words that the activity coefficient for a solvated proton SH^+ varies inversely with water concentration: $\gamma_{SH^+} \propto [H_2O]^{-1}$). If we assume that the same dependence holds for silanol protonation and take the activity coefficient into account, we predict that

$$\frac{k_{eff}}{\chi} = \frac{[HCl]}{[H_2O]}\{(k''_{cw} - 2k''_{ca})\chi + 2k''_{ca}\} \qquad (13)$$

or that:

$$\frac{k_{eff}[H_2O]}{\chi[HCl]} = (k''_{cw} - 2k''_{ca})\chi + 2k''_{ca} \qquad (14)$$

Figure 5 shows the results of fitting eq 14 to the experimental data. Surprisingly, the conclusion drawn when taking the dependence of the proton activity coefficient on water content into account is exactly the opposite from before. Again restricting the fit so that the *x*-intercept falls within reasonable bounds (≤ 0), we find that the *y*-intercept is approximately zero and that the slope is positive. In other words, alcohol-producing condensation appears to be negligible.

Given this large difference in the interpretation depending on the assumption about the activity of protonated silanols, one might wonder which result to believe. First of all, it is clear that, at high ethanol contents in ethanol/water mixtures containing hydrochloric acid, acid strength (as measured for instance by Hammett acidity[34]) decreases with increasing water content.[21,35] It would be unwise to ignore this effect as the water concentration varies over an order of magnitude (see Table 2). Also, we know that tetraethoxysilane does not interact strongly with ethanol,[36] so we have reason to expect that the presence of the organosilicon compounds does not strongly interfere with the acidity behavior observed in ethanol/water mixtures.

Therefore it appears that the initial conclusion that ethanol-producing condensation dominates (Figure 4) was incorrect. Since the free water concentration decreases with decreasing χ_{eq}, the increasing value of the ordinate (with decreasing χ_{eq}) in the figure is caused more by increased acid activity than the competition between condensation routes. Therefore, water-producing condensation is the most likely condensation route for trimethylsilanol in acidic ethanol/water mixtures. We are encouraged in this conclusion because Assink and Kay[23] found the same thing to be true in low-water tetraethoxysilane condensation. Kelling and coworkers[17] have reported that the rate of acid-catalyzed *methanol*-producing condensation of trimethylsilanols competes with that of water-producing condensation. However, if the rate coefficient for ethanol-producing condensation is over an order of magnitude lower than methanol-producing condensation (as it is under basic conditions[17]), water-producing condensation could indeed be dominant, as we have observed.

Alkaline System. The ^{29}Si NMR spectra collected for the alkaline sample (B-1 in Table 1) contain the same features as the acidic system. Trimethylethoxysilane, trimethylsilanol, and hexamethyldisiloxane are all present at approximately the same chemical shifts as under acidic conditions. The fraction of deprotonated silanols (discussed below) is too small to influence the chemical shift. We verified that the total integrated ^{29}Si NMR intensity remains constant during the course of reaction of the alkaline system.

The alkaline TMES system does not show instantaneous hydrolysis equilibrium like the acidic solutions do. Instead, Figure 6 shows that χ takes several minutes to reach a constant (equilibrium) value. Since we see a relatively slow hydrolysis transient, we comment on hydrolysis kinetics. We should be able to measure from the initial monomer decay a forward hydrolysis rate coefficient (k_h). However, hydrolysis is a little too fast for this: the extent of hydrolysis is over 60% by the first measured NMR spectrum. We can, however, place a lower bound on the hydrolysis rate coefficient using a simplified analysis of these data. Neglecting the effects of condensation on hydrolysis extent, we write

$$\frac{d[M_0^0]}{dt} = -k_h[H_2O][M_0^0] + k_e[EtOH][M_0^1] \qquad (15)$$

The water concentration is a function of time in this equation, but we can use the stoichiometry of the hydrolysis reaction to write

$$[H_2O](t) = [H_2O]_0 - [M_0^1](t)$$

and

$$[EtOH](t) = [EtOH]_0 + [M_0^1](t)$$

Substituting this in to eq 15 gives

$$\frac{d\chi}{dk_h[M_0]t} = W + \chi\left\{-(W+1) - \frac{E}{K_h} + \chi(1 - 1/K_h)\right\} \quad (16)$$

where χ is defined earlier, $W = [H_2O]_0/[M_0]$, $E = [EtOH]_0/[M_0]$, $K_h = k_h/k_e$, and $[M_0]$ is the total monomer concentration. Since W and E are fixed by our experiment, only K_h is truly adjustable on the right hand side of this equation. This equation is expressed in a dimensionless form. If it is valid, it should be possible to match the equation to the experimental data simply by (1) finding a K_h value consistent with the long-time behavior of the data and (2) finding a k_h value which scales the measured data to the numerical solution of this equation.

For the first step, we find that the long-time hydrolysis extent is consistent with $K_h = 18.5$. This value falls within the range of hydrolysis equilibrium coefficients measured previously.[12] For the second step of matching to the experimental data, we find that $k_h = 13\ M^{-1}\cdot h^{-1}$. An excellent match between the hydrolysis kinetics model and the data is shown in Figure 6. The estimate of k_h should be regarded as a lower bound, since some monomer is in fact being consumed during the approach to hydrolysis pseudoequilibrium.

Although the extent of hydrolysis is not constant, we should be able to use the measured values to find the condensation rate coefficient for this system. To do this, we go back to the equation we would write for the rate of decay of monomer by water-producing condensation:

$$\frac{d[M_0]}{dt} = -k_{cw}\chi^2[M_0]^2 \quad (17)$$

Earlier, we assumed that χ could be determined from an equilibrium coefficient or could be measured and was approximately constant. Since in this case χ does change with time, we simply retain the time dependence and solve the differential equation:

$$\frac{1}{[M_0]} - \frac{1}{[M_0]_0} = k_{cw}\int_0^t \chi^2(t')dt' \quad (18)$$

If the data vary slowly with time (and in this case they do), we can approximate the integral in this equation with a trapezoidal integration of the experimental data. We then expect a linear relationship between the inverse monomer concentration and this approximate integral. It turns out that this equation does not fit all of the experimental data, however (Figure 7). As the figure shows, a linear fit to the first data points fails to match the experimental data at longer times.

One reason eq 18 fails to match the measured data is that we have assumed that the rate coefficient is constant when in reality the composition of the solution changes with time. We can be sure that the observed deviation is not due to condensation reversibility because the slope of the curve increases with time; if reversibility were the problem, the rate would drop. The composition might, however, feed back to the condensation rate through a dependence on the concentration of ionic species. It has in fact been proposed that base-catalyzed condensation of silanols proceeeds through a deprotonated intermediate,[16,20] so

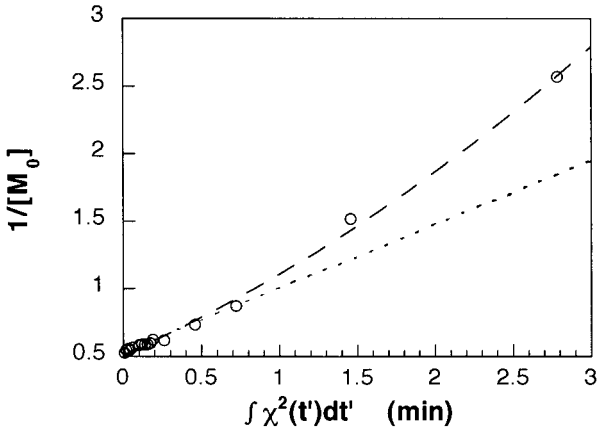

Figure 7. Relationship between inverse monomer concentration and integral of the square of hydrolysis extent for the base-catalyzed sample. The dashed line is a guide to the eye through the experimental data, and the dotted line is a linear fit to the first few data points.

that the rate of condensation is proportional to $[SiOH][SiO^-]$ rather than strictly to $[SiOH]^2$. The question, then, is whether the ratio of deprotonated species changes during reaction.

If deprotonation happens much more quickly than condensation, we can assume a deprotonation pseudoequilibrium for this system, which allows us to use our measured deprotonation coefficient to calculate the fraction of deprotonated silanols. We know the $K_d = 10$,[12] so we can write

$$\frac{[SiO^-][H_2O]}{[SiOH][OH^-]} = K_d = 10 \quad (19)$$

Neglecting deprotonated alcohol, we can approximate that all added sodium hydroxide is present either as a hydroxyl anion or as a silanol anion, in which case $[OH^-] + [SiO^-] = [NaOH]_0$. We also presume that the water concentration is known from the stoichiometry hydrolysis and condensation at each datum and that the NMR peak for hydrolyzed monomer includes both deprotonated and normal silanols ($[SiO^-] + [SiOH] = [Si]\chi(1-\alpha)$ where $\alpha = [M_1]/[Si]$). Substituting these relationships and solving the resulting quadratic equation gives

$$f_d = \frac{[SiO^-]}{([SiOH] + [SiO^-])} = \frac{([NaOH]_0 + [Si](1-\alpha)\chi + [H_2O]/10)}{2[Si](1-\alpha)\chi} - \frac{\sqrt{([NaOH]_0 + [Si](1-\alpha)\chi + [H_2O]/10)^2 - 4[NaOH]_0[Si](1-\alpha)\chi}}{2[Si](1-\alpha)\chi} \quad (20)$$

Does this equation predict that the fraction of deprotonated silanols changes significantly with time? We plot in Figure 8 the results of eq 20 applied to our data as a function of time. Clearly the fraction of deprotonated silanols is predicted to increase significantly after hydrolysis pseudoequilibrium is established, passing through a minimum at about 0.5 h and doubling from this value over the next four hours. This change could explain why the rate of condensation appears to increase with time.

Incorporating this value into our original expression from the condensation rate:

$$\frac{d[M_0]}{dt} = -k_{cw}^{\dagger} f_d(t)\chi^2(t)[M_0]^2(t)$$

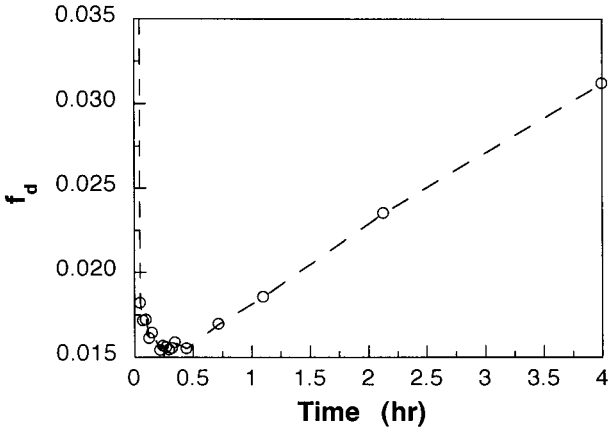

Figure 8. Fraction of deprotonated silanols in the base-catalyzed trimethylethoxysilane system as a function of time. The dashed line is provided as a guide to the eye.

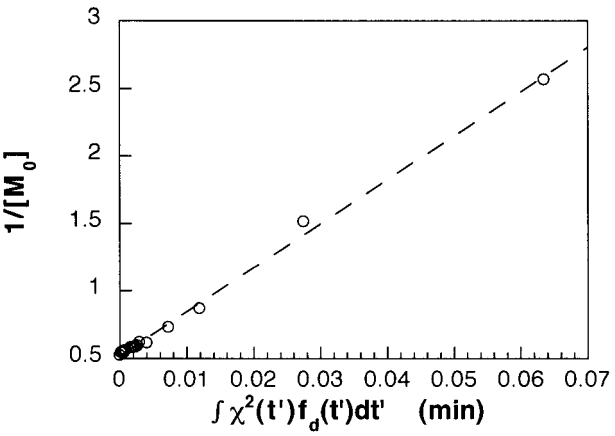

Figure 9. Plot of inverse monomer concentration as a function of the integral of the experimental product of the fraction of deprotonated silanols and the square of the hydrolysis extent for sample B-1. The dashed line is a least-squares fit to the data points.

Again, taking the measured values of f_d and χ at each point allows us to test the following relationship:

$$\frac{1}{[M_0]} - \frac{1}{[M_0]_0} = k_{cw}^{+} \int_0^t f_d(t')\chi^2(t')dt' \qquad (21)$$

Where the integral is approximated by trapezoidal integration of the experimental data plotted with respect to time.

Figure 9 shows that the relationship in eq 21 is able to match the experimental data with $k_{cw}^{+} = 32.6 \pm 0.5$ (M h)$^{-1}$. So unlike the acid-catalyzed case where the fraction of protonated silanols remains constant during reaction, we must account for the changing balance of deprotonation as a weak acid (silanol) is generated, titrated, and consumed during base-catalyzed hydrolytic condensation of trimethylethoxysilane.

The necessity of including this changing deprotonation may seem surprising compared to previous reports. Previously, it has been suggested that silanol homocondensation should be first order with respect to silanol and first order with respect to hydroxide anion.[14] This is actually a simplification of eq 20 and 21 when K_d is large enough and $[H_2O]$ is small enough that $[SiO^-] \sim [NaOH]_0$ at all times. Keeping the water content low is easy to do when one starts with silanols and works in nonalcoholic solvents. When ethanol is present, however, water is needed (due to esterification) to keep the hydrolysis extent high, so these conditions are not as easily met.

To see how our sample compares to those where first-order kinetics apply, we plot in Figure 10 the fraction of original

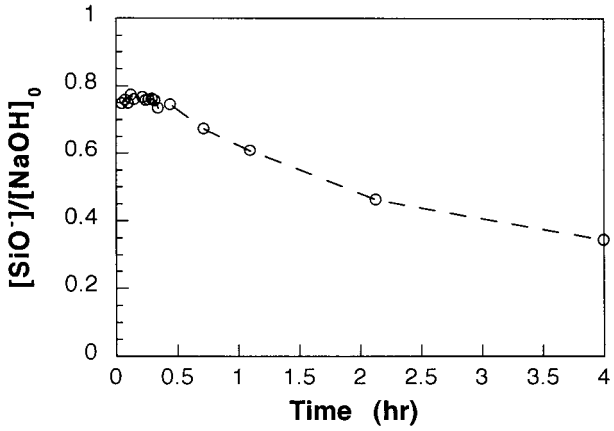

Figure 10. Fraction of NaOH consumed by silanols as a function of time for sample B-1. Dashed line is only a guide to the eye.

sodium hydroxide which is consumed by silanols. This fraction is not equal to one and is not even constant for our sample. If the silanol concentration were very large or if K_d were larger, the assumption of a constant deprotonated silanol concentration might be better met. This particular composition illustrates, however, why first-order kinetics have been observed under some but not all conditions for alkaline silanol condensation.

Conclusions

We have monitored the kinetics of hydrolytic dimerization of trimethylethoxysilane in nonideal conditions. The behavior in both acidic and basic solutions had to be analyzed with more complex models than had been used previously.

Under acidic conditions, facile hydrolysis pseudoequilibrium prevails in all samples. This makes it difficult to distinguish the route of condensation (alcohol vs water producing). By studying this monofunctional monomer, we have ruled out the possibility of substitution effects on reactivity. Accounting for the effect of addition of small amounts of water to mostly ethanol solutions (which tends to lower the activity of hydrogen ions), we have concluded that the water-producing route dominates the condensation of trimethylsilanol over a wide range of water concentrations (even if the net effect of water addition on condensation rate is negative).

Under alkaline conditions, we examined another common occurrence in realistic synthesis conditions: the use of a very high concentration of catalyst. First, we find that hydrolysis does reach pseudoequilibrium during the measured interval but more slowly than with acid. We also find that the deprotonation equilibrium shifts during reaction. The extent of deprotonation of the silanols passes through a minimum with respect to time; the subsequent increase in deprotonation leads to an *increase* in dimerization rate late in reaction. When we properly account for this, we are able to write a set of equations for trimethylethoxysilane hydrolytic dimerization with variable hydrolysis and deprotonation extents which matches the data.

Acknowledgment. The authors thank the Center for Interfacial Engineering at the University of Minnesota and Dow Corning Corporation for research support. S.E.R. also thanks the National Science Foundation and the University of Minnesota Graduate School for support through graduate fellowships. We thank Shayne Kirchner for preparing the base-catalyzed sample. We also thank Dr. Gary Wieber of Dow Corning for helpful discussions.

Appendix: Observation of Phase Separation

In one case noted in the text (sample A-5), the integrated intensity of the ^{29}Si NMR spectra did *not* remain constant. Figure

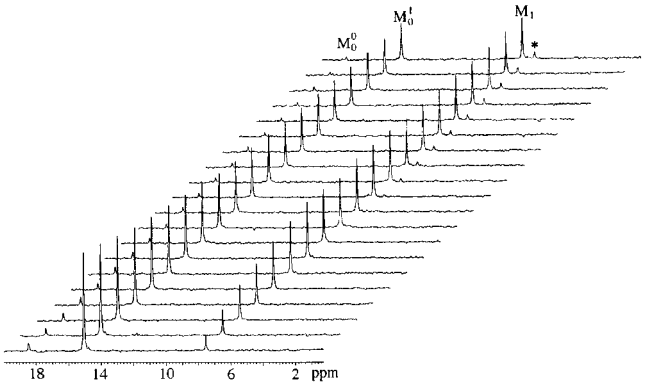

Figure 11. ^{29}Si NMR spectra collected for sample A-5. A totally new peak is observed (*) which has not previously been observed in homogeneous systems. The first spectrum is collected 3.2 min after mixing and 2.7 min evolve between spectra.

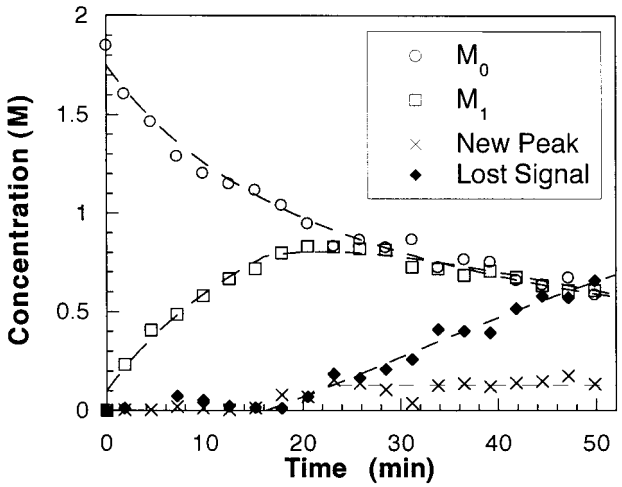

Figure 12. Plot of concentrations from ^{29}Si NMR data. Concentrations of M_0, M_1, and the new "mystery" species are determined by comparison to the intensity of a nonreactive monomer solution of equal concentration. The signal lost is the difference between the measured concentrations of M_0 and M_1 and the known silicon concentration.

11 shows how the spectra evolve. The peaks observed are nearly identical to those of the homogeneous monofunctional systems (although shifted somewhat due to the changed composition: +0.5 ppm for the silanol and +1 ppm for the ethoxysilane) with the important exception of one new peak (labeled with an asterisk in Figure 11). This peak appears slightly downfield of the dimer (M_1) peak, indicating nuclei in a better shielded environment.

At very long times compared to those shown in Figure 11, two distinct liquid phases can be observed in the sample. Neither phase contains a species giving the ^{29}Si NMR peak marked with an asterisk in Figure 11, so it is clear that this is an intermediate species. We can learn more about the nature of this species by examining the concentration transients of this sample.

Figure 12 shows how the concentrations of M_0 and M_1 vary with time, along with the concentration of the mystery species and the "lost" signal (the difference between the added silicon concentration and the measured concentrations of M_0 and M_1). These concentrations are determined by assuming that the absolute signal intensity measured by NMR is proportional to the number of silicon nuclei of that type present in the solution, an assumption justified normally because of complete relaxation between ^{29}Si pulses.

The monomer (M_0) concentration behaves just like the monomer concentration in a homogeneous system, showing the kind of decay expected for second-order kinetics. In fact, the curve passing through the data points in Figure 12 is a fit of the following function to the early-time data (up to 20 min of reaction):

$$[M_0] = \frac{[M_0]_0}{1 + k_{\text{eff}}[M_0]_o t} \tag{22}$$

Notice that the function continues to match to monomer concentration well even after the "mystery" species appears and the signal begins to be lost. That the monomer concentration does not decrease more quickly than homogeneous second-order kinetics would dictate suggests that the monomer is not part of the overall signal being lost from this sample.

The concentration of dimer (M_1) sites increases as expected for the first 20 min of reaction, but as soon as an appreciable concentration of the mystery peak appears, M_1 begins to disappear below the value expected by second-order kinetics. The curve passing through the M_1 data in Figure 12 is a fit of the following empirical function:

$$[M_1] = \begin{cases} [M_0]_0 - [M_0] & t < 18 \text{ min} \\ ([M_0]_0 - [M_0])\, e^{-k_{ps}(t-18 \text{ min})} & t \geq 18 \text{ min} \end{cases} \tag{23}$$

It is not clear how to interpret the ability of this function to fit the data. The exponential decay coefficient k_{ps} can be interpreted as a pseudo-first-order phase separation rate coefficient, but this does not have a rigorous physical justification.

Coincident with the loss of dimer signal near 20 min of reaction, the "mystery species" appears. The concentration of this species plateaus quickly, however, at a concentration of 0.125 M. Because this sample eventually forms two liquid phases, it seems reasonable that this new peak and the loss of M_1 signal represented in Figure 12 are both associated with the early stages of phase separation. Since M_0 does not disappear any more quickly than second-order kinetics would dictate at any time, it appears that the species being lost from the NMR spectra are mainly M_1 sites. Three factors may contribute to loss of signal from M_1 in this newly formed phase. (1) Presuming that the new phase is less polar than the majority of the solution, the relaxation agent (chromium acethylacetonate) may partition preferentially in the polar phase. Decreased relaxation in the new apolar phase would lead to easier spin saturation and eventually to loss of signal compared to the signal expected from fully-relaxed nuclei. (2) The new apolar phase is of lower density and may migrate out of the measurement volume (the sample is large enough for this to occur). (3) The new apolar phase might be initially present in small domains in which molecular motion is restricted, leading to slowed spin-lattice relaxation (due to inhibited molecular tumbling) and to broadening of the signal.

Since the new "mystery" peak appears as phase separation occurs, it most likely arises from M_1 sites in a new environment, possibly on the surface of the domains of the new phase or in nuclei of the new phase.

While the details of what is going on in sample A-5 are not entirely clear, it is evident that some sort of phase separation is occurring after 20 min of reaction, leading to loss of NMR signal. Since this system does not produce solid precipitates, this demonstrates that the formation of a solid phase is not necessary to explain loss of ^{29}Si NMR signal in sol-gel solutions. This suggests that, in alkoxysilane systems that do form particles, the observed loss of NMR signal upon phase separation[37] could happen as soon as liquid−liquid phase separation

begins and does not require exceptionally fast condensation in the newly formed phase to explain the lack of intermediates and products in the liquid-satate ^{29}Si NMR spectra.

One final note: if the new peak we observe in the ^{29}Si NMR spectra is a good indicator of phase separation, it appears that one point on the two-phase boundary of this multicomponent system is (the composition at 20 min) 54 mol % ethanol, 40 mol % water, 0.31 mol % trimethylethoxyilane, 3.6 mol % trimethylsilanol, and 1.7 mol % hexamethyldisiloxane (with 0.0023 M HCl).

References and Notes

(1) Brinker, C. J.; Scherer, G. W. *Sol-gel Science: The Physics and Chemistry of Sol-Gel Processing*; Academic Press: Boston, 1990.

(2) Mark, J. E.; Lee, C. Y.-G.; Bianconi, P. A., Eds. *Hybrid Inorganic-Organic Composites*; American Chemical Society: Washington, DC, 1995.

(3) Schaefer, D. W.; Wilkes, G. L.; Sanchez, C.; Coltrain, B., Eds. *Better Ceramics Through Chemistry VII*; Materials Research Society: Pittsburgh, PA, 1996.

(4) Mann, S.; Burkett, S. L.; Davis, S. A.; Fowler, C. E.; Mendelson, N. H.; Sims, S. D.; Walsh, D.; Whilton, N. T. *Chem. Mater.* **1997**, *9*, 2300.

(5) Navrotsky, A. Thermochemistry of Crystalline and Amorphous Silica. In *Silica: Physical Behavior, Geochemistry and Materials Applications*; Heaney, P. J., Prewitt, C. T., Gibbs, G. V. G., Eds.; Mineralogical Society of America: Washington, DC, 1994.

(6) Brunet, F.; Cabane, B.; Dubois, M.; Perly, B. *J. Phys. Chem.* **1991**, *95*, 945.

(7) Sanchez, J.; McCormick, A. V. *J. Phys. Chem.* **1992**, *96*, 8973.

(8) Friberg, S. E.; Yang, J.; Amran, A.; Sjöblom, J.; Farrington, G. *J. Phys. Chem.* **1994**, *98*, 13528.

(9) Ng, L. V.; McCormick, A. V. *J. Phys. Chem.* **1996**, *100*, 12517.

(10) Fyfe, C. A.; Aroca, P. P. *J. Phys. Chem. B* **1997**, *101*, 9504.

(11) By distribution, we refer not only to size differences but also to structural differences. For instance, polycyclic silicates are likely to be very important in the stability of acid-catalyzed sol−gel systems.

(12) Šefčík, J.; Rankin, S. E.; Kirchner, S. J.; McCormick, A. V. *J. Non-Cryst. Solids* **1999**. Manuscript submitted for publication.

(13) Grubb, W. T. *J. Am. Chem. Soc.* **1954**, *76*, 3408.

(14) Rutz, W.; Lange, D.; Kelling, H. *Z. Anorg. Allg. Chem.* **1985**, *528*, 98.

(15) Bilda, S.; Lange, D.; Popowski, E.; Kelling, H. *Z. Anorg. Allg. Chem.* **1987**, *550*, 186.

(16) Bilda, S.; Lange, D.; Popowski, E.; Kelling, H. *Z. Anorg. Allg. Chem.* **1988**, *564*, 155.

(17) Spitzner, H.; Wandschneider, S.; Lange, D.; Kelling, H. *J. Prakt. Chem.* **1996**, *338*, 376.

(18) Pohl, E. R.; Osterholtz, F. D. Kinetics and mechanism of aqueous hydrolysis and condensation of alkyltrialkoxysilanes. In *Molecular Characterization of Composite Interfaces*; Ishida, H., Kumar, G., Eds.; Plenum Press: New York, 1985.

(19) Pohl, E. R.; Osterholtz, F. D. Kinetics and mechanism of condensation of alkylsilanols in aqueous solution. In *Silanes, Surfaces, and Interfaces*; Leyden, D. E., Ed.; Gordon and Breach: New York, 1986.

(20) Osterholtz, F. D.; Pohl, E. R. Kinetics of the hydrolysis and condensation of organofunctional alkoxysilanes: a review. In *Silanes and Other Coupling Agents*; Mittal, K., Ed.; VSP: Utrecht, 1992.

(21) Popovych, O.; Tomkins, R. P. T. *Nonaqueous Solution Chemistry*; Wiley: New York, 1981.

(22) Assink, R. A.; Kay, B. D. *J. Non-Cryst. Solids* **1988**, *99*, 359.

(23) Assink, R. A.; Kay, B. D. *Coll. Surf. A* **1993**, *74*, 1.

(24) Harris, R. K. *Nuclear Magnetic Resonance Spectroscopy. A Physicochemical View*; Wiley: New York, 1986.

(25) This peak ($\sim$ 110 ppm) is far from the peaks of TMES and its condensation products, but we collected spectra with the broad silica peak to avoid base line distortion by folding that peak into the measured spectra.

(26) Suda, S.; Iwaida, M.; Yamashita, K.; Umegaki, T. *J. Non-Cryst. Solids* **1994**, *176*, 26.

(27) Hook, R. J. *J. Non-Cryst. Solids* **1996**, *192*, 1.

(28) Williams, E. A.; Cargioli, J. D.; LaRochelle, R. W. *J. Organomet. Chem.* **1976**, *108*, 153.

(29) Rankin, S. E.; Macosko, C. W.; McCormick, A. V. *Mat. Res. Soc. Symp. Proc.* **1996**, *435*, 113.

(30) Rankin, S. E.; Šefčík, J.; McCormick, A. V. *Ind. Eng. Chem. Res.* **1999**. Manuscript submitted for publication.

(31) Crow, E. L.; Davis, F. A.; Maxfield, M. W. *Statistics Manual*; Dover, New York, 1960.

(32) This is justified by the observations that basicities of silanols and alcohols are comparable[33] (so $K_p \sim 1$) and that the concentration of silanol groups is at the very most one fifth the concentration of ethanol for any of these solutions. If S refers to water, K_p would be expected to be very small.

(33) West, R.; Baney, R. H. *J. Amer. Chem. Soc.* **1959**, *81*, 6145.

(34) Tourky, A. R.; Abdel-Hamid, A. A.; Slim, I. Z. *Z. Phys. Chem. Leipzig* **1972**, *250*, 49.

(35) Tremillon, B. *Chemistry in Non-Aqueous Solvents*; D. Reidel: Boston, 1974 (in English).

(36) Saeten, J. O.; Selle, M. H.; Sjöblom, J.; Friberg, S. E.; Gestblom, B. *J. Solution Chem.* **1991**, *20*, 1149.

(37) Lee, K.; Look, J. L.; Harris, M. T.; McCormick, A. V. *J. Coll. Int. Sci.* **1997**, *194*, 78.